0026-895X/88/050651-08$02.00/0

MOLECULAR PHARMACOLOGY, 34:651-658

Iodination of [Tyr^{11}]Somatostatin Yields a Super High Affinity Ligand for Somatostatin Receptors in GH_4C_1 Pituitary Cells

DAVID H. PRESKY[1] and AGNES SCHONBRUNN[2]

Department of Pharmacology, Harvard Medical School, and Laboratory of Toxicology, Harvard School of Public Health, Boston, Massachusetts 02115

Received March 10, 1988; Accepted August 2, 1988

SUMMARY

GH_4C_1 cells are a clonal strain of rat pituitary tumor cells which contain high affinity receptors for the inhibitory neuropeptide somatostatin (SRIF). In contrast to other peptides that bind to specific receptors on these cells, receptor-bound [^{125}I-Tyr^1]SRIF does not undergo rapid endocytosis. Rather, partial degradation to ^{125}I-tyrosine occurs concommitantly with the dissociation of [^{125}I-Tyr^1]SRIF from cell surface receptors. In this study we characterize the binding, biological activity and receptor-mediated degradation of [^{125}I-Tyr^{11}]SRIF, a SRIF analog that is radiolabeled in the center of the molecule. The binding of trace concentrations of [^{125}I-Tyr^{11}]SRIF (<50 pM) required 6 hr to reach equilibrium at 37° compared with the 60 min required for [^{125}I-Tyr^1]SRIF. Analysis of the kinetics of [^{125}I- Tyr^{11}]SRIF binding showed that the rate constant for association (k_{on} = 1.7 × 10^8 $M^{-8}min^{-1}$) was similar to that for [^{125}I-Tyr^1]SRIF (0.8 × 10^8 $M^{-1}min^{-1}$). However, the two radioligands exhibited markedly different dissociation kinetics; the k_{off} for [^{125}I-Tyr^{11}]SRIF was 0.002 min^{-1} compared with the value of 0.02 min^{-1} for [^{125}I-Tyr^1]SRIF. In agreement with its much slower rate of dissociation, [^{125}I-Tyr^{11}]SRIF bound to the SRIF receptor with higher affinity (K_d = 70 pM) than did [^{125}I-Tyr^1]SRIF (K_d = 350 pM). However, the apparent ED_{50} for [I-Tyr^{11}]SRIF to inhibit cAMP accumulation (1.9 ± 0.4 nM) was greater than the ED_{50} for SRIF (0.19 ± 0.04 nM). The low potency of [I-Tyr^{11}]SRIF probably resulted from the fact that subsaturating concentrations of this peptide did not achieve equilibrium binding during the 30-min incubation used to assay biological activity. As previously reported for [^{125}I-Tyr^1]SRIF, receptor-bound [^{125}I-Tyr^{11}]SRIF was not internalized and was released from the cells as a mixture of intact [^{125}I-Tyr^{11}]SRIF (30%) and the degradation product ^{125}I-tyrosine (65%). Only ≈5% of receptor-bound [^{125}I-Tyr^{11}]SRIF was released as a different degradation product. Our data demonstrate that [^{125}I-Tyr^{11}]SRIF is a better radioanalog than [^{125}I-Tyr^1]SRIF for binding studies with intact cells because of its higher affinity for the SRIF receptor. In addition, inasmuch as receptor-mediated degradation of bound ligand releases iodotyrosine from both position 1 and position 11 substituted analogs, aminopeptidases are unlikely to be entirely responsible for SRIF degradation. The superior binding properties of [^{125}I-Tyr^{11}]SRIF should facilitate the detection of SRIF receptors in other cell types.

Recent structure-activity studies using different radiolabelled analogs of SRIF have indicated the existence of multiple SRIF receptor subtypes in brain (1–4) as well as in other tissues (5–10). Most of these studies have been carried out using membrane preparations. Furthermore, the membranes used were derived from tissues consisting of a mixture of target cells for SRIF and thus in some, if not all, instances, contain more than one type of SRIF receptor. A comparison of the binding and receptor-mediated processing of two different radiolabelled somatostatin analogs by intact cells has not been reported.

The GH_4C_1 pituitary cell line contains a single class of high affinity membrane receptors for SRIF which mediate the inhibitory effects of this tetradecapeptide on prolactin and growth hormone secretion (11–14). Interestingly, [^{125}I-Tyr^1]SRIF is so far unique among all peptide hormones and growth factors which bind to specific GH cell receptors in that it is not rapidly internalized (15). Nonetheless, a fraction of receptor-bound peptide is degraded to ^{125}I-tyrosine by a non-lysosomal process which appears to occur at the cell surface (15). The simplest mechanism by which this degradation could occur is cleavage of the amino terminal tyrosine leaving the 13-amino acid COOH-terminal peptide intact and biologically active. To determine whether degradation occurred in this manner, we examined the binding and receptor-mediated processing of the internally

This investigation was supported by a research grant from the National Institute of Arthritis, Diabetes, Digestive and Kidney Diseases (DK 32234). D.H.P. was partially supported by a National Research Service Award training grant (5 T32 GM07306) and a fellowship from the Albert J. Ryan Foundation, Cincinatti, Ohio.

[1] Present address: Laboratory of Immunology, National Institute of Allergy and Infectious Diseases, National Institutes of Health, Building 10 Room 11N311, Bethesda, MD 20892.

[2] Present address: Department of Pharmacology, University of Texas Medical School, P. O. Box 20708, Houston, TX 77225.

ABBREVIATIONS: SRIF, somatostatin; HEPES, 4(2-hydroxyethyl)-1-piperazine-ethane-sulfonic acid; HEPES-F10-lh, Ham's F10 medium without bicarbonate supplemented with 5 mg/ml lactalbumin hydrolysate and 20 mM HEPES, pH 7.4; TFA, trifluoroacetic acid; VIP, vasoactive intestinal peptide; HPLC, high performance liquid chromatography.

labelled SRIF analog [^{125}I-Tyr^{11}]SRIF in intact GH_4C_1 cells. This radioligand has been reported to be more useful than [^{125}I-Tyr^{1}]SRIF for measuring SRIF receptors in membrane preparations because of its decreased susceptibility to proteolysis (10, 16). The results presented here demonstrate that [^{125}I-Tyr^{11}]SRIF is also a much better radioligand than [^{125}I-Tyr^{1}]SRIF for binding studies with intact GH cells. However, this is due to its 10-fold higher affinity for the SRIF receptor rather than to its greater stability.

Experimental Procedures

Materials. Materials were obtained from the following sources: synthetic SRIF, [Tyr^{1}]SRIF, and [Tyr^{11}]SRIF from Bachem (Torrance, CA); tyrosine and HEPES from Sigma Chemical Co. (St. Louis, MO); Na^{125}I (17 Ci/mg) and lactalbumin hydrolysate from ICN (Irvine, CA); Ham's F10 culture medium and sera from GIBCO (Grand Island, NY); and culture plates from Falcon Labware (Oxnard, CA). Dicarboxymethyl SRIF was the kind gift of Drs. P. Bacha and S. Reichlin, Tufts New England Medical Center (Boston, MA).

Cell culture. The properties of the GH_4C_1 clonal rat pituitary cell strain and the method of its culture have been described previously (17, 18). Experiments were performed using cells grown on either 35 mm dishes or 24-well culture plates (16-mm wells) as described previously (15).

Iodination of peptides and tyrosine. [^{125}I-Tyr^{1}]SRIF and [^{125}I-Tyr^{11}]SRIF were prepared by Chloramine T iodination as described previously (14). For both radiolabeled analogs, the reaction mixture was purified by reverse phase HPLC using a Supelco Supelcosil LC-18 column (25 cm × 4.6 mm) eluted at a flow rate of 0.5 ml/min with a 120-min linear gradient from 0.1% TFA to 0.1% TFA in 80% acetonitrile. This purification procedure completely separates iodinated from uniodinated peptide and therefore yields [^{125}I-Tyr^{1}]SRIF and [^{125}I-Tyr^{11}]SRIF with specific activities of 2200 Ci/mmol.

Nonradioactive [I-Tyr^{11}]SRIF was prepared by a modification of the radioiodination protocol described above. [Tyr^{11}]SRIF (500 μg) in 0.5 ml of 0.1 N hydrochloric acid was added to 110 μg of NaI in 1.7 ml of 0.5 M sodium phosphate, pH 7.5. Chloramine T (500 μg in 500 μl of water) was then added and the reaction was terminated after 15 sec with 300 μl of 1 mM tyrosine. The reaction mixture was purified on a Supelco Supelcosil LC-18 reverse phase column (25 cm × 4.6 mm) eluted at a flow rate of 1 ml/min with a 90 min linear gradient from 0.1% TFA in 20% acetonitrile to 0.1% TFA in 80% acetonitrile. Reaction products were detected by monitoring the absorbance at 280 nm. The retention times for the following standards were determined: ^{125}I-tyrosine, 8 min; [Tyr^{11}]SRIF, 36 min; [^{125}I-Tyr^{11}]SRIF, 44 min. Fractions comigrating with [^{125}I-Tyr^{11}]SRIF were pooled and the concentration of [I-Tyr^{11}]SRIF was determined by amino acid analysis of samples subjected to 4 hr hydrolysis in 6 N hydrochloric acid at 145° *in vacuo* courtesy of Dr. B. Perelle, Harvard Medical School (Boston, MA). Additional samples of [I-Tyr^{11}]SRIF were a generous gift from Dr. J. Rivier, Salk Institute, San Diego, CA. ^{125}I-Tyrosine was prepared by chloramine T iodination as described previously (19).

Measurement of peptide binding to cells. All binding studies were performed using a modification of the procedure of Schonbrunn and Tashjian (14) in which incubations were carried out in Ham's F10 medium supplemented with 5 mg/ml lactalbumin hydrolysate and buffered to pH 7.4 with 20 mM HEPES (HEPES-F10-Ih). Except where noted, all reported values represent saturable peptide binding, which was calculated by subtracting the amount of peptide bound in the presence of 100 nM SRIF (nonsaturable binding) from the amount of peptide bound in the absence of any unlabelled peptide (total binding). Nonsaturable binding represented 25–30% and 5–10% of total binding for [^{125}I-Tyr^{1}]SRIF and [^{125}I-Tyr^{11}]SRIF, respectively. In some experiments the procedure of Haigler *et al.* (20) was used to remove surface-bound peptide by incubation with 0.2 M acetic acid, 0.5 M NaCl, pH 2.5, at 4° as described previously (15).

Measurement of cAMP accumulation. The effect of SRIF analogs on cAMP production was determined as described previously (21). Briefly, after a 30-min preincubation with 250 μM 3-isobutyl-1-methyl xanthine, GH_4C_1 cells were incubated for another 30 min in fresh HEPES-F10-Ih containing 250 μM 3-isobutyl-1-methyl xanthine, 100 nM VIP, and the indicated concentration of SRIF analog. The amount of cAMP accumulated in the medium during the second 30-min incubation at 37° was measured by radioimmunoassay. Under these conditions changes in extracellular cAMP concentrations parallel effects on intracellular cAMP levels (22).

HPLC analysis of [^{125}I-Tyr^{11}]SRIF degradation. Aliquots of HEPES-F10-Ih dissociation medium were injected onto a Supelco Supelcosil LC-18 column (25 cm × 4.6 mm) and eluted at a flow rate of 1 ml/min with a 45-min linear gradient from 0.1% TFA to 0.1% TFA in 80% acetonitrile. One-minute fractions were collected and the amount of radioactivity present in each fraction was determined. [^{125}I-Tyr^{11}]SRIF and ^{125}I-tyrosine standards were run under identical conditions as the media samples. Recoveries of ^{125}I from the column were greater than 90%.

Data analysis. For determination of saturable peptide binding, the standard error was calculated by taking the square root of the sum of the squares of the standard errors for total and nonsaturable binding. Because GH_4C_1 cells contain a single class of noninteracting SRIF receptors (14), dose-response and equilibrium binding data were fit to a rectangular hyperbola by a nonlinear regression program (procedure NLIN; Statistical Analysis System, SAS Institute, Cary, NC). Dissociation curves were fit to a single exponential decay by the same program. Values for ED_{50}, K_d, B_{max}, and half-times are given with their standard errors. The Cheng-Prusoff equation (23) was used to calculate K_d from the observed IC_{50} in competition binding experiments. All experiments were conducted at least three times. Error bars not shown are within the size of the symbol.

Results

Time course of [^{125}I-Tyr^{11}]SRIF binding. The time course of [^{125}I-Tyr^{11}]SRIF binding to GH_4C_1 cells is shown in Fig. 1. The amount of saturably bound [^{125}I-Tyr^{11}]SRIF increased with time and reached a plateau after 6 hr at 37°. At steady state, saturable binding represented 95% of total binding. In contrast, the binding of [^{125}I-Tyr^{1}]SRIF under identical conditions reaches a plateau after only 1 hr (14). To determine whether this difference in binding kinetics was a result of differences in

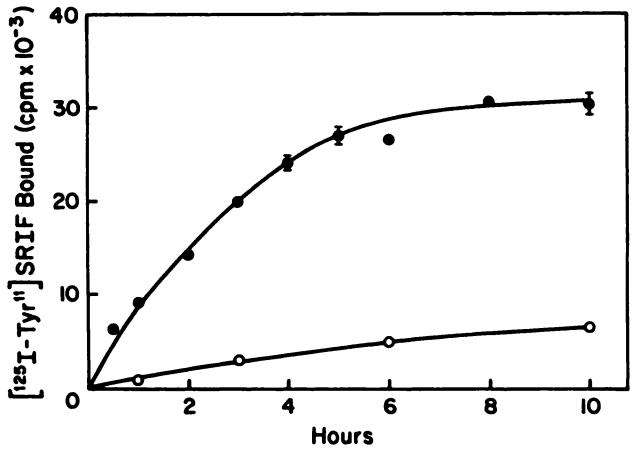

Fig. 1. Time course of [^{125}I-Tyr^{11}]SRIF binding. GH_4C_1 cells (1.1 × 10^6 cells/dish) were incubated at 37° in 2 ml of HEPES-F10-Ih containing 124,000 cpm/ml (42 pM) of [^{125}I-Tyr^{11}]SRIF in the absence and presence of 100 nM SRIF. At the indicated time, both total (●) and acid/salt-resistant (○) [^{125}I-Tyr^{11}]SRIF binding was determined. *Error bars* represent the standard error of triplicate determinations.

processing of receptor-bound ligand, we examined the subcellular distribution of saturably bound [^{125}I-Tyr^{11}]SRIF after different periods of binding using the acid wash protocol of Haigler *et al.* (20) (Fig. 1). This procedure permits surface-bound hormone to be distinguished from internalized hormone (20). At all times examined greater than 80% of the saturably bound [^{125}I-Tyr^{11}]SRIF was removed by extracting the cells with 0.2 M acetic acid, 0.5 M NaCl, pH 2.5 (acid/salt) for 5 min at 4°. These results paralleled those with [^{125}I-Tyr^{1}]SRIF (15) and indicated that the slow binding kinetics observed with [^{125}I-Tyr^{11}]SRIF were not due to time-dependent intracellular accumulation of internalized peptide.

Concentration dependence of [^{125}I-Tyr^{11}]SRIF binding. The binding of [^{125}I-Tyr^{11}]SRIF to GH_4C_1 cells at equilibrium exhibited dose dependence with the characteristics expected for the binding of homogeneous radiolabeled peptide to a single class of noninteracting binding sites (Fig. 2). The K_d for [^{125}I-Tyr^{11}]SRIF was 199,000 ± 8,000 cpm/ml, which corresponds to 68 ± 3 pM. Scatchard analysis of the binding data demonstrated that the number of binding sites/cell was 11,100 ± 160 (Fig. 2). In three independent experiments with different preparations of [^{125}I-Tyr^{11}]SRIF, the K_d was determined to be 72 ± 4 pM, and the B_{max} was 12,350 ± 1,200 sites/cell. The number of [^{125}I-Tyr^{11}]SRIF binding sites is in agreement with the 8,800 ± 2,100 binding sites per GH_4C_1 cell for [^{125}I-Tyr^{1}]SRIF (14). The high affinity observed for [^{125}I-Tyr^{11}]SRIF, however, was unexpected. Previous studies in GH_4C_1 cells gave a K_d of 1.7 nM for the uniodinated peptide [Tyr^{11}]SRIF (12).

The differences in the binding affinities as well as the rates of approach to equilibrium for [^{125}I-Tyr^{1}]SRIF and [^{125}I-Tyr^{11}]SRIF could be explained by the two radiolabeled ligands binding to separate populations of SRIF receptors. Although this seemed unlikely because the number of binding sites for the two ligands were the same, we further examined this possibility by determining the concentration dependence for SRIF inhibition of both [^{125}I-Tyr^{1}]SRIF and [^{125}I-Tyr^{11}]SRIF binding. The data presented in Fig. 3 show that in the absence of any SRIF the amount of saturably bound radiolabeled peptide differed markedly for the two analogs. This difference in the level of saturable binding could be attributed to the differences in the affinity of the two radioligands for the SRIF receptor, 70 pM for [^{125}I-Tyr^{11}]SRIF and 350 pM for [^{125}I-Tyr^{1}]SRIF (14). Nonetheless, SRIF competed for the binding of the two radiolabeled analogs with similar potencies. After correcting the observed IC_{50} values using the Cheng-Prusoff equation (23) to yield the true K_d for unlabelled SRIF, the calculated binding affinity for SRIF was found to be independent of the radiolabelled analog used in the competition experiment. In replicate experiments, the observed K_d values for SRIF were 276 ± 19 pM (six experiments) and 285 ± 33 pM (four experiments), calculated from the inhibition of [^{125}I-Tyr^{1}]SRIF and [^{125}I-Tyr^{11}]SRIF binding, respectively.

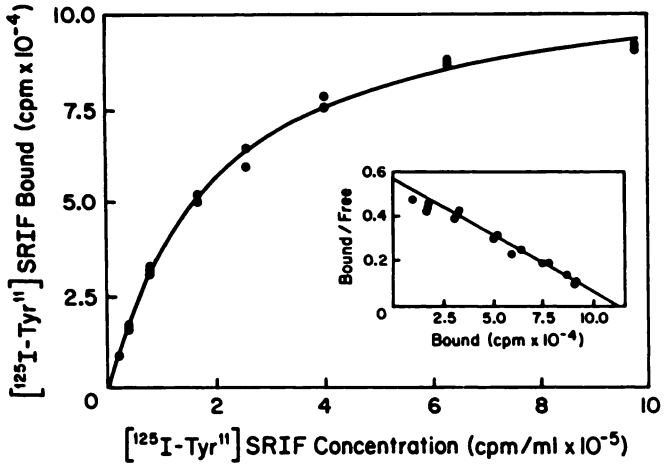

Fig. 2. Concentration dependence for [^{125}I-Tyr^{11}]SRIF binding. GH_4C_1 cells (2.1 × 10^6 cells/dish) were incubated in 1 ml of HEPES-F10-Ih containing the indicated concentration of [^{125}I-Tyr^{11}]SRIF in the absence and presence of 100 nM SRIF. After 8 hr at 37° saturable [^{125}I-Tyr^{11}] SRIF binding was determined as described in Experimental Procedures. The computer-fitted regression lines are shown and were determined as described in Experimental Procedures. *Inset*, binding data were plotted by the method of Scatchard (22).

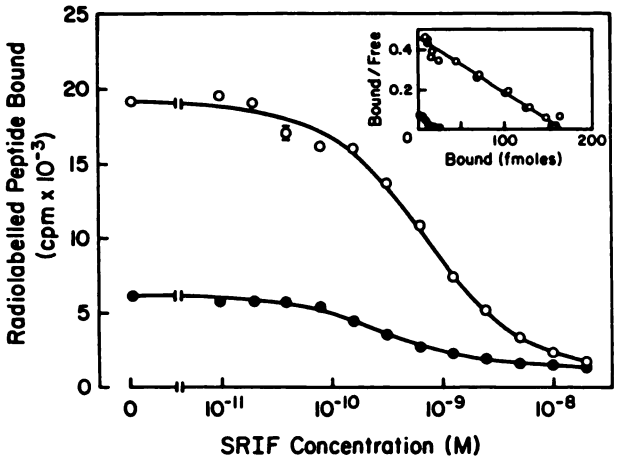

Fig. 3. Concentration dependence for the inhibition of [^{125}I-Tyr^{1}]SRIF and [^{125}I-Tyr^{11}]SRIF binding by SRIF. GH_4C_1 cells (1.2 × 10^6 cells/dish) were incubated at 37° in 2 ml of HEPES-F10-Ih containing the indicated concentration of SRIF and either [^{125}I-Tyr^{1}]SRIF (67,000 cpm/ml) (●) or [^{125}I-Tyr^{11}]SRIF (59,000 cpm/ml) (○). At the end of the binding incubation, which was 60 min for [^{125}I-Tyr^{1}]SRIF and 8 hr for [^{125}I-Tyr^{11}]SRIF, the amount of bound radiolabeled peptide was determined. *Error bars* represent the range of duplicate determinations and the *lines* represent computer-fitted regression lines determined as described in Experimental Procedures. *Inset*, Binding data were plotted by the method of Scatchard (22).

In contrast to the identical binding affinities obtained for SRIF from competition data with [^{125}I-Tyr^{11}]SRIF and [^{125}I-Tyr^{1}]SRIF, Scatchard (24) analysis yielded very different values for the maximum number of binding sites. The results presented in Fig. 3 *inset* gave a B_{max} of 10,990 ± 900 sites/cell from the inhibition of [^{125}I-Tyr^{1}]SRIF binding and a B_{max} of 87,420 ± 9,420 sites/cell from the inhibition of [^{125}I-Tyr^{11}]SRIF binding. However, this apparent discrepancy in the maximal binding capacities can be explained by the differing affinities of the two radioligands used. The assumption usually made when calculating the maximal binding capacity by dilution with unlabeled peptide is that the affinities of the radiolabeled (K_d^*) and unlabeled (K_d) peptides are identical. However when the K_d^* is much smaller than the K_d, the x intercept of the Scatchard plot (B_{max}) will be: $B_{max} = R \times K_d/K_d^*$ (25). For [^{125}I-Tyr^{1}]SRIF, K_d^* is essentially equal to the K_d for SRIF and the observed x intercept of the Scatchard plot in Fig. 3 therefore gives the density of SRIF receptors. For [^{125}I-Tyr^{11}]SRIF, however, K_d^* is much smaller than the K_d for SRIF and consequently the x intercept of the Scatchard plot is greater than that observed with [^{125}I-Tyr^{1}]SRIF. After correcting for differences in K_d^* and

K_d, the number of SRIF binding sites determined with the two ligands were similar.

The fact that SRIF inhibited the binding of both ligands with the same potency suggested that the two radioanalogs bound to the same receptor population. This conclusion was supported by a number of additional observations as follows: (i) [Tyr^{11}]SRIF, as well as SRIF, inhibited the binding of [^{125}I-Tyr^{1}]SRIF and [^{125}I-Tyr^{11}]SRIF with similar potencies (Fig. 4) (12). Furthermore, dicarboxymethyl SRIF, a nonoxidizable, linear SRIF derivative, was at least 100-fold less potent than SRIF for inhibiting [^{125}I-Tyr^{11}]SRIF binding consistent with the observation that reduced, linear derivatives of SRIF are much less potent than SRIF at displacing [^{125}I-Tyr^{1}]SRIF from GH_4C_1 cells (12). (ii) Both [Tyr^{1}]SRIF and Tyr^{11}]SRIF were able to completely inhibit saturable [^{125}I-Tyr^{1}]SRIF and [^{125}I-Tyr^{11}]SRIF binding (Fig. 4) (14). In addition, 100 nM [I-Tyr^{11}] SRIF completely inhibited the binding of [^{125}I-Tyr^{1}]SRIF as well as [^{125}I-Tyr^{11}]SRIF. (iii) [^{125}I-Tyr^{11}]SRIF did not bind to saturable receptors on GH_4C_1 cells, a sub-clone of GH_4C_1 cells that does not exhibit either [^{125}I-Tyr^{1}]SRIF binding or a biological response to SRIF (14). Together, these data provide strong support for the conclusion that [^{125}I-Tyr^{11}]SRIF binds to the same population of SRIF receptors as does [^{125}I-Tyr^{1}] SRIF.

Kinetics of [^{125}I-Tyr^{11}]SRIF binding. To determine whether changes in the association or dissociation rate constants were responsible for the higher binding affinity of [^{125}I-Tyr^{11}]SRIF than of [^{125}I-Tyr^{1}]SRIF, we compared the association and dissociation kinetics of the two radioligands. We measured the initial rate of [^{125}I-Tyr^{11}]SRIF binding to determine its association rate constant (Fig. 5). The value for k_{on} was calculated using the equation: $k_{on} \equiv v_i/(L^* \times R)$ where v_i is the initial velocity of the binding reaction, L^* is the concentration of [^{125}I-Tyr^{11}]SRIF, and R is the concentration of SRIF receptors. Linear regression analysis of the initial 10 min of binding yielded a bimolecular rate constant, k_{on}, of 1.5×10^8 $M^{-1}min^{-1}$ (Fig. 5). In three separate experiments using different preparations of [^{125}I-Tyr^{11}]SRIF, the calculated k_{on} was 1.73 ± 0.12 × 10^8 $M^{-1}min^{-1}$. This is similar to the k_{on} of 7.7×10^7 $M^{-1}min^{-1}$ for [^{125}I-Tyr^{1}]SRIF binding to GH_4C_1 cells as determined by Schonbrunn and Tashjian (14).

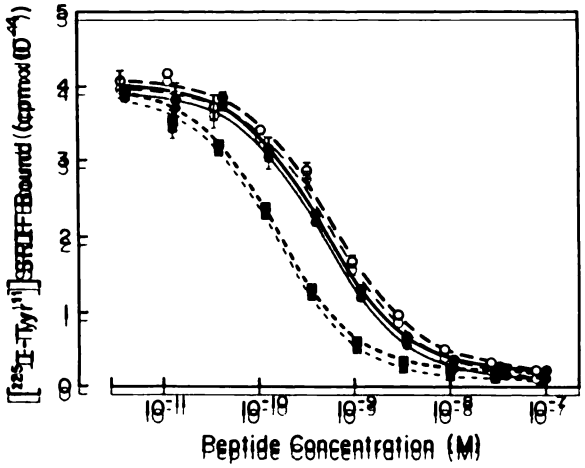

Fig. 4. Concentration dependence for the inhibition of [^{125}I-Tyr^{11}]SRIF binding by SRIF analogs. GH_4C_1 cells (1.4×10^6 cells/dish) were incubated at 37° with [^{125}I-Tyr^{11}]SRIF (149,000 cpm/ml) and the indicated concentration of SRIF (●), [Tyr^{11}]SRIF (○), or [I-Tyr^{11}]SRIF (■). After 2 hr the amount of bound [^{125}I-Tyr^{11}]SRIF was determined as described in Experimental Procedures. *Error bars* represent the range of duplicate determinations and the lines represent computer-fitted regression lines determined as described in Experimental Procedures.

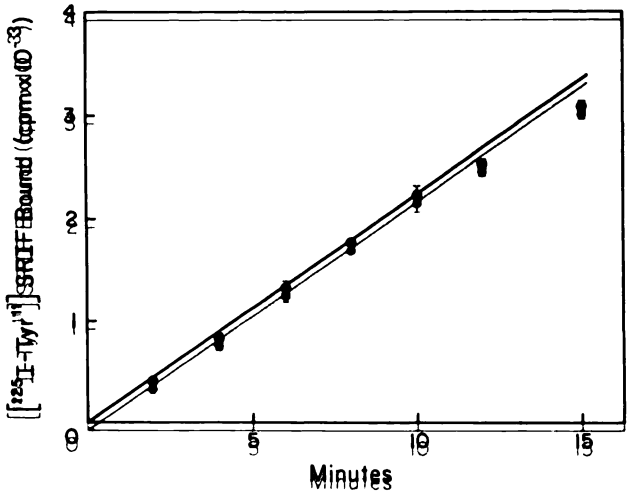

Fig. 5. Initial rate of [^{125}I-Tyr^{11}]SRIF binding. GH_4C_1 cells (2.0×10^6 cells/dish) were incubated at 37° with 2 ml of HEPES-F10-H containing 40,000 cpm/ml (14 pM) of [^{125}I-Tyr^{11}]SRIF in the absence and presence of 100 nM SRIF. At the indicated times saturable [^{125}I-Tyr^{11}]SRIF binding was determined as described in Experimental Procedures. The receptor concentration was calculated to be 19 pM by Scatchard analysis of the concentration dependence for [^{125}I-Tyr^{11}]SRIF binding in replicate cultures. *Error bars* represent the standard error of triplicate determinations and the *line* represents the computer-fitted regression line determined as described in Experimental Procedures.

The dissociation of receptor-bound [^{125}I-Tyr^{11}]SRIF followed first-order kinetics with a half-time of 6.1 ± 0.3 hr (k_{off} of 1.9 ± 0.09 × 10^{-3}min^{-1}) (Fig. 6A). In five independent experiments the k_{off} was 2.03 ± 0.58 × 10^{-3}min^{-1}. The rate of [^{125}I-Tyr^{11}] SRIF dissociation was unaffected by the presence of 100 nM SRIF in the dissociation medium ($k_{off} \equiv 2.15 \pm 0.08 \times 10^{-3}$min^{-1}) (Fig. 6B), consistent with an absence of cooperativity in [^{125}I-Tyr^{11}]SRIF binding. In addition, the dissociation kinetics were the same, independent of whether equilibrium binding had been reached or the dissociation reaction was initiated before equilibrium ($k_{off} \equiv 1.96 \pm 0.23 \times 10^{-3}$min^{-1}). This last result showed that a time-dependent shift in the k_{off} of the receptor did not occur (Fig. 6B). The dissociation rate constant for [^{125}I-Tyr^{11}]SRIF (2.0×10^{-3}min^{-1}) was considerably smaller than the dissociation rate constant for [^{125}I-Tyr^{1}] SRIF determined under identical conditions (2.3×10^{-2} min^{-1}) (14). Table 1 summarizes the kinetic constants for the binding of [^{125}I-Tyr^{1}]SRIF and [^{125}I-Tyr^{11}]SRIF to GH_4C_1 cells at 37°. These results demonstrate that the increased affinity of [^{125}I-Tyr^{11}]SRIF compared with [^{125}I-Tyr^{1}]SRIF was primarily due to a slower rate of dissociation for [^{125}I-Tyr^{11}]SRIF.

Concentration dependence for SRIF and [I-Tyr^{11}] inhibition of cAMP accumulation. Dorflinger and Schonbrunn (22) have shown that SRIF inhibits VIP-stimulated cAMP accumulation in GH_4C_1 cells, an activity that results in SRIF inhibition of VIP stimulated prolactin secretion (11). To determine whether the high binding affinity of [I-Tyr^{11}]SRIF caused it to be a super active SRIF agonist, we determined its potency to inhibit hormone-stimulated cAMP accumulation using our previous assay conditions (21). The results in Fig. 7 show that the ED_{50} for [I-Tyr^{11}]SRIF inhibition of cAMP accumulation was 1.9 ± 0.4 nM, a value substantially below the ED_{50} for native SRIF (0.19 ± 0.04 nM). Furthermore, the ED_{50}

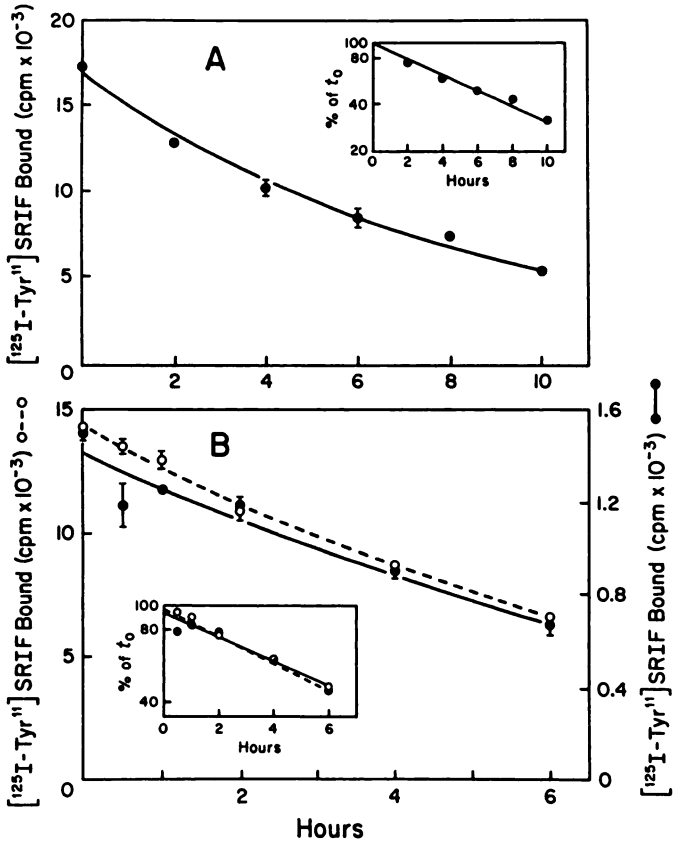

Fig. 6. Time course of [^{125}I-Tyr^{11}]SRIF dissociation. A, GH_4C_1 cells were incubated for 7 hr at 37° in 1 ml of HEPES-F10-Ih containing [^{125}I-Tyr^{11}]SRIF (175,000 cpm/ml) in the absence and presence of 100 nM SRIF. The cells were then rinsed with 4° saline and 1 ml of 37° HEPES-F10-Ih was added to each dish (t = 0). The amount of saturably bound [^{125}I-Tyr^{11}]SRIF remaining after various periods of time at 37° was determined as described in Experimental Procedures. *Error bars* represent the standard error of triplicate determinations and the *line* represents the computer-fitted regression line. B, Identical to A except that either the binding incubation was carried out for 10 min at 37° (●, *right axis*) or that 100 nM SRIF was present during the dissociation incubation (○, *left axis*).

TABLE 1

Summary of rate and equilibrium constants for [^{125}I-Tyr^1]SRIF and [^{125}I-Tyr^{11}]SRIF binding to GH_4C_1 cells

Values represent mean ± standard error of at least three determinations.

	Ligand	
	[^{125}I-Tyr^1]SRIF	[^{125}I-Tyr^{11}]SRIF
k_{on} (M^{-1} min^{-1})	$7.7 \pm 0.9 \times 10^{7a}$	$1.7 \pm 0.7 \times 10^{8}$
k_{off} (min^{-1})	$2.3 \pm 0.2 \times 10^{-2a}$	$2.0 \pm 0.6 \times 10^{-3}$
K_d (M)	$3.5 \pm 0.8 \times 10^{-10a}$	$7.2 \pm 4.0 \times 10^{-11}$
K_d for SRIF (M)	$2.8 \pm 0.2 \times 10^{-10}$	$2.9 \pm 0.3 \times 10^{-10}$

[a] Determined under identical conditions by Schonbrunn and Tashjian (14).

for [I-Tyr^{11}]SRIF to inhibit cAMP accumulation was significantly higher than its potency to inhibit [^{125}I-Tyr^{11}]SRIF binding (Fig. 4; calculated K_d = 0.07 nM).

One possible explanation for the discrepancy between the measured binding affinity and biological potency of [I-Tyr^{11}]SRIF could be that this analog did not achieve equilibrium binding during the relatively short duration of the cAMP accumulation experiments (30 min). Under preequilibrium conditions the dose-response curve for the peptide would be expected to be shifted to higher concentrations than observed in

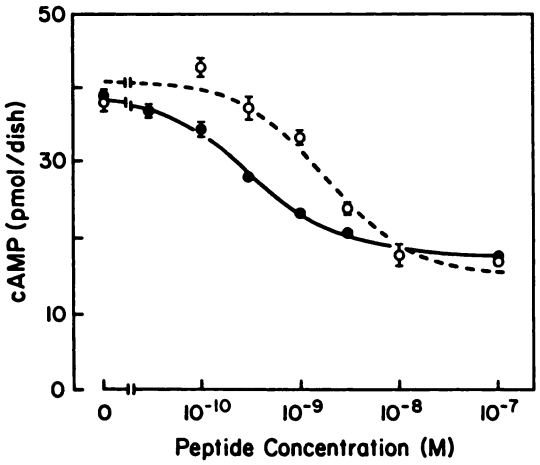

Fig. 7. Concentration dependence for inhibition of cAMP accumulation by [I-Tyr^{11}]SRIF. GH_4C_1 cells were incubated for 30 min at 37° in HEPES-F10-Ih containing 250 μM isobutylmethyl xanthine, 100 nM VIP, and the indicated concentration of SRIF (●) or [I-Tyr^{11}]SRIF (○). The amount of cAMP accumulated in the medium was determined by radioimmunoassay. *Error bars* represent the standard error of triplicate determinations and the *lines* represent computer-fitted regression lines.

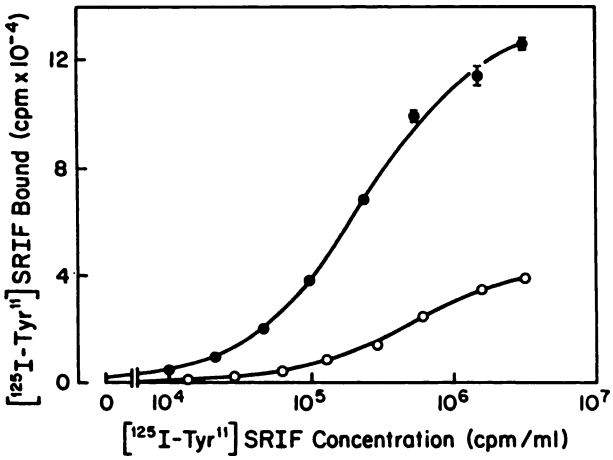

Fig. 8. Concentration dependence for [^{125}I-Tyr^{11}]SRIF binding after different incubation times. GH_4C_1 cells were incubated at 37° for either 8 hr (●) or 30 min (○). The incubation was carried out both with and without 100 nM SRIF in HEPES-F10-Ih containing the indicated concentration of [^{125}I-Tyr^{11}]SRIF. At the end of the binding reaction, saturable [^{125}I-Tyr^{11}]SRIF binding was determined as described in Experimental Procedures. *Error bars* represent the standard error of triplicate determinations and the *lines* represent computer-fitted regression lines. One nanomolar SRIF corresponds to 3.2×10^6 cpm/ml.

equilibrium binding studies. To address this possibility directly, we compared the concentration dependence of [^{125}I-Tyr^{11}]SRIF binding during the preequilibrium conditions normally used for the cAMP assay (30 min incubation at 37°) and during conditions that allowed equilibrium binding to be established (8 hr at 37°) (Fig. 8). As expected, the 30-min incubation produced much lower binding than the 8-hr incubation. In fact the dose-response curves were shifted about 30-fold (Fig. 8). These results support the conclusion that the 27-fold difference between the K_d for [I-Tyr^{11}]SRIF (0.07 nM) and its potency to inhibit cAMP accumulation (ED_{50} = 1.9 nM) is due to the differences in the duration of the experiments in which these parameters were measured.

Degradation of receptor-bound [^{125}I-Tyr^1]SRIF. GH_4C_1 cells degrade about half of receptor-bound [^{125}I-Tyr^1]

SRIF to ^{125}I-tyrosine (15). To gain further insight into the mechanism of this receptor-mediated degradation, we examined the form in which [^{125}I-Tyr^{11}]SRIF was released from the receptor. [^{125}I-Tyr^{11}]SRIF was incubated with cells at 37°, unbound material was washed away, and the radioactivity released from the cells during subsequent incubations at 37° was collected and analyzed by reverse phase HPLC (Fig. 9). As previously seen with receptor-bound [^{125}I-Tyr^{1}]SRIF, the principal degradation product comigrated with ^{125}I-tyrosine. However, a small peak of radioactivity was eluted between ^{125}I-tyrosine and intact [^{125}I-Tyr^{11}]SRIF with a retention time of 26 min (P26).

The nature of the radioactivity released from the cells after different periods of dissociation is presented in Table 2. About 30% of total radioactivity was intact peptide at all time points examined. As with [^{125}I-Tyr^{1}]SRIF, degradation was receptor-mediated and not simply due to instability of the radioligand; [^{125}I-Tyr^{11}]SRIF incubated with cells during the binding incubation (5 hr at 37°) remains greater than 90% intact. Further, the presence of 100 nM SRIF in the dissociation medium had only a slight effect on the degradation process. Finally, 97% of the [^{125}I-Tyr^{11}]SRIF that remains bound to the cells after a 6-hr dissociation incubation chromatographed as intact peptide, demonstrating that degraded radioligand does not remain bound to the cells and that degradation occurs essentially simultaneously with dissociation. These results show that despite the very different dissociation kinetics of [^{125}I-Tyr^{1}]SRIF and [^{125}I-Tyr^{11}]SRIF, the two peptides are processed similarly following receptor binding.

Discussion

It is known that membrane receptors that are linked to guanyl nucleotide-binding proteins can behave differently when examined in intact cells versus membrane preparations (26–28). In particular, such receptors have been more difficult to characterize by agonist binding to whole cells than to membranes because of the lower affinity form of the receptor present in the whole cell preparation. SRIF receptors are known to be coupled to a pertussis toxin-sensitive guanyl nucleotide-binding protein (13, 29, 30). Therefore, it is not altogether surprising that characterization of high affinity SRIF receptors in whole cells has been reported for only a few systems (14, 32–34) whereas SRIF receptors have been described in membranes prepared from a number of target tissues (10). In this study, we demonstrate that [^{125}I-Tyr^{11}]SRIF is a superior radioanalog compared with [^{125}I-Tyr^{1}]SRIF for studying the SRIF receptor in intact GH cells by virtue of its higher level of saturable binding. Thus, this ultra-high affinity ligand markedly increases the sensitivity of the SRIF binding assay. Although there is no guarantee that this will hold true for SRIF receptors in other cell types, we have recently used this ligand to characterize β cell SRIF receptors which were present in such low concentrations (1000 sites/cell) as to be barely detectable with [^{125}I-Tyr^{1}]SRIF (34, 35).

The binding of [^{125}I-Tyr^{11}]SRIF occurred more slowly and reached a higher plateau at steady state than the binding of [^{125}I-Tyr^{1}]SRIF. Two possible explanations for these differences were examined. First, the processing of receptor-bound [^{125}I-Tyr^{11}]SRIF was investigated to determine if the increased binding of [^{125}I-Tyr^{11}]SRIF might be due to receptor-mediated uptake of the radioligand. However, as had been seen with [^{125}I-Tyr^{1}]SRIF, greater than 80% of saturably bound [^{125}I-Tyr^{11}]SRIF was removed by acid/salt extraction at all time points indicating the absence of [^{125}I-Tyr^{11}]SRIF uptake. Second, we examined the possible existence of a separate pool of SRIF receptors accessible only to [Tyr^{11}]SRIF analogs. This pool could have missed detection with [^{125}I-Tyr^{1}]SRIF as the radi-

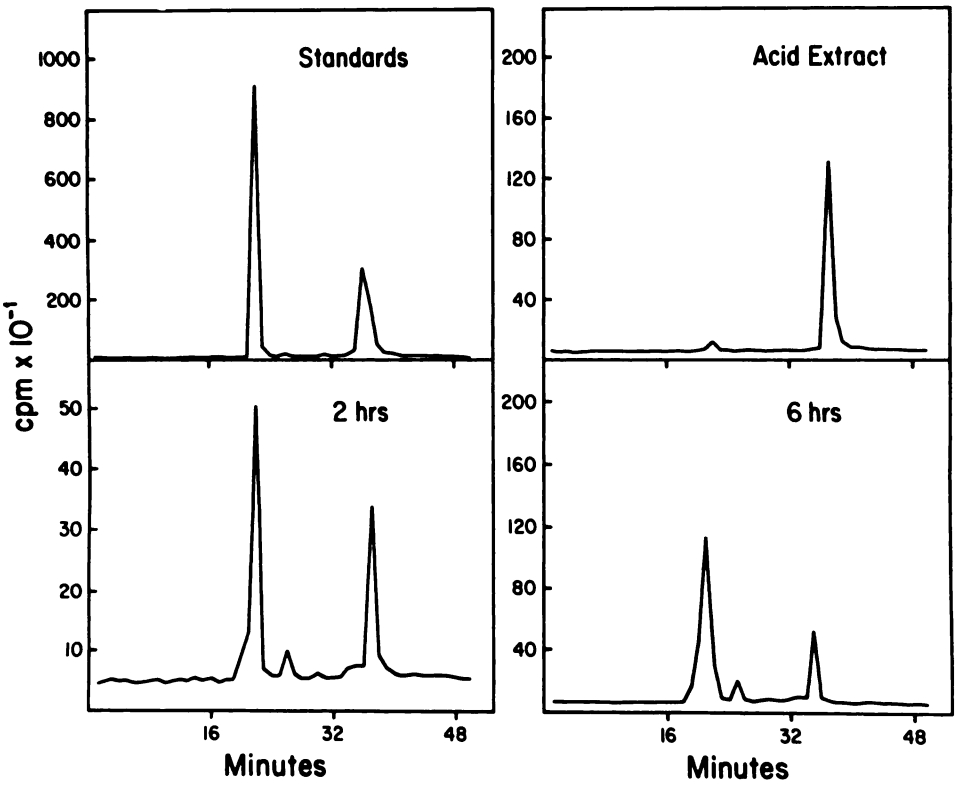

Fig. 9. Chromatographic analysis of the degradation products produced from receptor-bound [^{125}I-Tyr^{11}]SRIF. GH_4C_1 cells were incubated for 5 hr at 37° in HEPES-F10-Ih containing [^{125}I-Tyr^{11}]SRIF (276,000 cpm/ml) in the absence and presence of 100 nM SRIF. The cells were then incubated for 30 min at 37° with 1 ml of HEPES-F10-Ih to allow 70% of the nonsaturably bound [^{125}I-Tyr^{11}]SRIF to dissociate. During this 30-min wash period only 8% of saturably bound [^{125}I-Tyr^{11}]SRIF dissociated. At this point the amount of saturably bound [^{125}I-Tyr^{11}]SRIF was 39,740 ± 620 cpm/dish and represented 95% of total binding. One milliliter of fresh HEPES-F10-Ih was then added (t = 0), and the cells were incubated at 37° for either 2 or 6 hr. The amount of saturably bound [^{125}I-Tyr^{11}]SRIF released into the dissociation medium was determined (see Table 2) and aliquots of the binding and dissociation media were analyzed by reverse phase HPLC as described in Experimental Procedures. Dishes labeled *Acid Extract* were extracted with acid/salt, pH 2.5 after a 6-hr dissociation incubation and the acid extract was analyzed by reverse phase HPLC. The panel labeled *Standards* shows the elution of ^{125}I-tyrosine (21 min) and [^{125}I-Tyr^{11}]SRIF (36 min). Recovery of injected ^{125}I was always greater than 90%.

TABLE 2

Degradation of receptor-bound [^{125}I-Tyr^{11}]SRIF

GH_4C_1 cells were incubated with [^{125}I-Tyr^{11}]SRIF for 5 hr at 37° and then washed with HEPES-F10-Ih as described in the legend to Fig. 9. Saturable binding of [^{125}I-Tyr^{11}]SRIF was 39,740 ± 620 cpm at this time and represented 95% of the total bound peptide. Subsequently, the cells were transferred into 1 ml of fresh HEPES-F10-Ih and the amount of saturably bound [^{125}I-Tyr^{11}]SRIF released into the medium was measured after the times shown. SRIF (100 nM) was added to the dissociation incubation for the group specified. Samples labeled Acid Extract were obtained by extracting the cells with acid/salt, pH 2.5, for 5 min at 37° after a 6-hr dissociation incubation at 37°. Aliquots of media and the acid/salt extract were analyzed by reverse phase HPLC as described in Experimental Procedures. The data show the percentage of the total ^{125}I injected that comigrated with ^{125}I-tyrosine or [^{125}I-Tyr^{11}]SRIF standards, as well as that which eluted with a retention time of 26 min (P26).

Sample	^{125}I Released[a]	^{125}I-Tyrosine[b]	P_{26}[b]	[^{125}I-Tyr^{11}]SRIF[b]
	cpm/dish		*% of total ^{125}I*	
Binding medium		6 ± 1	1 ± 1	93 ± 1
2 hr	7,176 ± 195	63 ± 3	4 ± 1	32 ± 3
4 hr	13,829 ± 579	67 ± 1	4 ± 1	28 ± 1
6 hr	17,406 ± 990	69 ± 4	7 ± 2	24 ± 3
6 hr + 100 nM SRIF	18,758 ± 201	62 ± 1	5 ± 1	33 ± 1
6 hr, acid extract	16,648 ± 512	3 ± 0	0	97 ± 0

[a] Mean ± standard error of triplicate determinations.
[b] Mean ± standard error of duplicate determinations.

oligand and thus could account for the increased binding of [^{125}I-Tyr^{11}]SRIF. However, several observations indicate that this is not the case. [Tyr^1]SRIF completely inhibited the binding of [^{125}I-Tyr^{11}]SRIF and [I-Tyr^{11}]SRIF completely inhibited [^{125}I-Tyr^1]SRIF binding. In addition, SRIF and [Tyr^{11}]SRIF competed for the binding of the two radioligands with the same potencies. Finally, GH_4C_1 cells have the same number of receptors for [^{125}I-Tyr^1]SRIF and [^{125}I-Tyr^{11}]SRIF whereas a subclone of GH cells previously shown to lack receptors for [^{125}I-Tyr^1]SRIF ($GH_{12}C_1$) also did not bind [^{125}I-Tyr^{11}]SRIF. Thus, both radioligands must bind to one common pool of SRIF receptors and the increased binding of [^{125}I-Tyr^{11}]SRIF is explained by its increased affinity for that receptor pool.

The high affinity of [^{125}I-Tyr^{11}]SRIF was unexpected because we previously found that the affinity of the uniodinated peptide, [Tyr^{11}]SRIF, is somewhat lower than that of SRIF and [^{125}I-Tyr^1]SRIF (12). Apparently iodination of the Tyr^{11} residue, which increases the hydrophobicity of the phenoxy ring and lowers the pK_a of the hydroxyl group, increased the affinity of [Tyr^{11}]SRIF for the SRIF receptor. Whereas iodination often reduces the affinity of peptides for their receptors, it has been reported to increase the binding affinity of glucagon (36, 37).

Examination of the kinetics of [^{125}I-Tyr^{11}]SRIF binding revealed that the increased affinity of [^{125}I-Tyr^{11}]SRIF compared with [^{125}I-Tyr^1]SRIF was due primarily to differences in the dissociation kinetics of the two radioligands; [^{125}I-Tyr^{11}]SRIF dissociated 10 times more slowly than [^{125}I-Tyr^1]SRIF. The smaller k_{off} for [^{125}I-Tyr^{11}]SRIF also explains the long time necessary for [^{125}I-Tyr^{11}]SRIF binding to reach equilibrium, because the rate of approach to equilibrium (k_{obs}) for a bimolecular reaction is a function of k_{off}, as well as k_{on} and the concentration of the radioligand (14): $k_{obs} = k_{on} \times [L^*] + k_{off}$

The fact that [I-Tyr^{11}]SRIF required prolonged incubations to reach equilibrium complicated the experiments aimed at determining its biological potency. In contrast to its higher binding affinity relative to SRIF, measured in experiments carried out at equilibrium, [I-Tyr^{11}]SRIF was less potent than SRIF at acutely inhibiting VIP-stimulated cAMP production. Binding experiments employing a short incubation period supported the conclusion that the unexpectedly low potency of [I-Tyr^{11}]SRIF in acute experiments was probably due to the fact that equilibrium binding was not achieved during the biological assay. These results clearly show that kinetics of receptor binding, as well as equilibrium binding affinities, contribute to the biological activities of peptide agonists.

Despite the large differences in the rates of dissociation of [^{125}I-Tyr^1]SRIF and [^{125}I-Tyr^{11}]SRIF, the processing of the two peptides was remarkably similar. In parallel with the results reported for [^{125}I-Tyr^1]SRIF (15), receptor-bound [^{125}I-Tyr^{11}]SRIF was not internalized and underwent partial degradation during dissociation from the cell surface. The primary degradation product in the dissociation medium was ^{125}I-tyrosine, although a small amount of material that did not comigrate with either intact [^{125}I-Tyr^{11}]SRIF or ^{125}I-tyrosine was also present and may represent a short-lived intermediate product. The fact that ^{125}I-tyrosine was the principal degradation product of [^{125}I-Tyr^{11}]SRIF suggests that aminopeptidases are not solely responsible for receptor-mediated proteolysis. In addition, it indicates that the initial cleavage step is rate limiting in the degradation of [^{125}I-Tyr^{11}]SRIF to ^{125}I-tyrosine.

It is known that the biological responses to SRIF do not desensitize upon chronic treatment of GH_4C_1 cells with the peptide (21). However, the biological actions of SRIF are reversed within minutes after its removal from normal rat pituitary cells (38, 39). Our binding experiments raise the interesting possibility that [I-Tyr^{11}]SRIF may be a particularly long acting analog of SRIF.

References

1. Reubi, J. C. Evidence for two somatostatin-14 receptor types in rat brain cortex. *Neurosci. Lett.* **49:** 259–263 (1984).
2. Reubi, J. C. New specific radioligand for one subpopulation of brain somatostatin receptors. *Life Sci.* **36:** 1829–1836 (1985).
3. Tran, V. T., M. F. Beal, and J. B. Martin. Two types of somatostatin receptors differentiated by cyclic somatostatin analogs. *Science (Wash. D. C.)* **228:** 492–495 (1985).
4. Heiman, M. L., W. A. Murphy, and D. H. Coy. Differential binding of somatostatin agonists to somatostatin receptors in brain and adenohypophysis. *Neuroendocrinology* **45:** 429–436 (1987).
5. Brown, M., J. Rivier, and W. Vale. Somatostatin analogs with selected biological activities. *Science (Wash. D. C.)* **196:** 1467–1469 (1977).
6. Meyers, C. A., D. H. Coy, W. A. Murphy, T. W. Redding, A. Arimura, and A. V. Schally. [Phe^4]Somatostatin: a potent, selective inhibitor of growth hormone release. *Proc. Natl. Acad. Sci. USA* **77:** 577–579 (1980).
7. Srikant, C. B., and Y. C. Patel. Somatostatin receptors in the rat adrenal cortex: characterization and comparison with brain and pituitary receptors. *Endocrinology* **116:** 1717–1723 (1985).
8. Srikant, C. B., and Y. C. Patel. Somatostatin analogs: dissociation of brain receptor binding affinities and pituitary actions in the rat. *Endocrinology* **108:** 341–343 (1981).
9. Srikant, C. B., and S. Heisler. Relationship between receptor binding and biopotency of somatostatin-14 and somatostatin-28 in mouse pituitary tumor cells. *Endocrinology* **117:** 271–278 (1985).
10. Srikant, C. B., and Y. C. Patel. Somatostatin receptors, in *Somatostatin* (Y. C. Patel and G. S. Tannenbaum, eds.). Plenum Press, New York, 291–304 (1985).
11. Schonbrunn, A., and B. D. Koch. Mechanisms by which somatostatin inhibits pituitary hormone release in *Samatostatin, Basic and Clinical Status.* (S. Reichlin, ed.). Plenum Press, New York, 121–135 (1987).
12. Schonbrunn, A., O. P. Rorstad, J. M. Westendorf, and J. B. Martin. Somatostatin analogs: correlation between receptor binding affinity and biological potency in GH pituitary cells. *Endocrinology* **113:** 1559–1567 (1983).
13. Koch, B. D., and A. Schonbrunn. The somatostatin receptor is directly coupled to adenylate cyclase in GH_4C_1 pituitary cell membranes. *Endocrinology* **114:** 1784–1790 (1984).
14. Schonbrunn, A., and A. H. Tashjian, Jr. Characterization of functional receptors for somatostatin in rat pituitary cells in culture. *J. Biol. Chem.* **253:** 6473–6483 (1978).
15. Presky, D. H., and A. Schonbrunn. Receptor-bound somatostatin and epidermal growth factor are processed differently in GH_4C_1 rat pituitary cells. *J. Cell Biol.* **102:** 878–888 (1986).
16. Srikant, C. B., and Y. C. Patel. Somatostatin receptors: identification and characterization in rat brain membranes. *Proc. Natl. Acad. Sci. USA* **78:** 3930–3934 (1981).

17. Tashjian, A. H., Jr., Y. Yasumura, L. Levine, G. H. Sato, and M. L. Parker. Establishment of clonal strains of rat pituitary tumor cells that secrete growth hormone. *Endocrinology* **82:** 342–352 (1968).
18. Bancroft, F. C. GH Cells: functional clonal lines of rat pituitary tumor cells, in *Functionally Differentiated Cell Lines* (G. Sato, ed), Alan R. Liss, New York, 47–59 (1982).
19. Westendorf, J. M., and A. Schonbrunn. Characterization of bombesin receptors in a rat pituitary cell line. *J. Biol. Chem.* **258:** 7527–7535 (1983).
20. Haigler, H. T., F. R. Maxfield, M. C. Willingham, and I. Pastan. Dansylcadaverine inhibits internalization of ^{125}I-epidermal growth factor in Balb 3T3 cells. *J. Biol. Chem.* **255:** 1239–1244 (1980).
21. Presky, D. H., and A. Schonbrunn. Somatostatin pretreatment increases the number of somatostatin receptors in GH_4C_1 pituitary cells and does not reduce cellular responsiveness to somatostatin. *J. Biol. Chem.* **263:** 714–721 (1988).
22. Dorflinger, L. J., and A. Schonbrunn. Somatostatin inhibits vasoactive intestinal peptide-stimulated cyclic adenosine monophosphate accumulation in GH pituitary cells. *Endocrinology* **113:** 1541–1550 (1983).
23. Cheng, Y.-C., and W. H. Prusoff. Relationship between the inhibition constant (K_i) and the concentration of inhibitor which causes 50 per cent inhibition (IC_{50}) of an enzymatic reaction. *Biochem. Pharmacol.* **22:** 3099–3108 (1973).
24. Scatchard, G. The attractions of proteins for small molecules and ions. *Ann. N.Y. Acad. Sci.* **51:** 660–672 (1949).
25. Taylor, S. I. Binding of hormones to receptors. An alternative explanation of nonlinear Scatchard plots. *Biochemistry* **14:** 2357–2361 (1975).
26. Pittman, P. C., and Molinoff, P. B. Interactions of agonists and antagonists with β adrenergic receptors on intact L6 muscle cells. *J. Cyclic Nucleotide Res.* **6:** 421–435 (1980).
27. Insel, P. A., L. C. Mahan, H. J. Motulsky, L. M. Stoolman, and A. M. Koachman. Time-dependent decreases in binding affinity of agonists for beta-adrenergic receptors of intact S49 lymphoma cells. *J. Biol. Chem.* **258:** 13597–13605 (1983).
28. Sladeczek, F., J. Bockaert, and J.-P. Mauger. Differences between agonist and antagonist binding to alpha1-adrenergic receptors of intact and broken-cell preparations. *Mol. Pharmacol.* **24:** 392–397 (1983).
29. Enjalbert, A. R. Rasolonjanahary, E. Moyse, C. Kordon, and J. Epelbaum. Guanine sensitivity of [^{125}I]-Iodo-N-Tyr somatostatin binding in rat adenohypophysis and cerebral cortex. *Endocrinology* **113:** 822–824 (1983).
30. Koch, B. D., L. J. Dorflinger, and A. Schonbrunn. Pertussis toxin blocks both cyclic AMP-mediated and cyclic AMP-independent actions of somatostatin: evidence for coupling of Ni to decreases in intracellular free calcium. *J. Biol. Chem.* **260:** 13138–13145 (1985).
31. Reisine, T., Y.-L. Zhang, and R. Sekura. Pertussis toxin treatment blocks the inhibition of somatostatin and increases the stimulation by forskolin of cyclic AMP accumulation and adrenocorticotropin secretion from mouse anterior pituitary cells. *J. Pharmacol. Exp. Ther.* **232:** 275–282 (1985).
32. Richardson, U. I., and A. Schonbrunn. Inhibition of adrenocorticotropin secretion by somatostatin in pituitary cells in culture. *Endocrinology* **108:** 281–290 (1981).
33. Esteve, J. P., C. Susini, N. Vaysse, H. Antoniotti, E. Wunsch, G. Berthon, and A. Ribet. Binding of somatostatin to pancreatic acinar cells. *Am. J. Physiol.* **247:** G62–G69 (1984).
34. Bhathena, S. J., H. K. Oie, A. E. Gazdar, N. R. Voyles, S. D. Wilkins, and L. Recant. Insulin, glucagon, and somatostatin receptors on cultured cells and clones from rat islet cell tumor. *Diabetes* **31:** 521–531 (1982).
35. Sullivan, S. J., and A. Schonbrunn. Characterization of somatostatin receptors which mediate inhibition of insulin secretion in RINm5F insulinoma cells. *Endocrinology* **121:** 544–552 (1987).
36. Lin, M. C., S. Nicosia, and M. Rodbell. Effects of iodination of tyrosyl residues on the binding and action of glucagon at its receptor. *Biochemistry* **15:** 4537–4540 (1976).
37. Rojas, F. J., T. L. Swartz, R. Iyengar, A. J. Garber, and L. Birnbaumer. Monoiodoglucagon: synthesis, purification by high pressure liquid chromatography, and characteristics as a receptor probe. *Endocrinology* **113:** 711–719 (1983).
38. Kraicer, J., and A. E. H. Chow. Release of growth hormone from purified somatotrophs: Use of perifusion system to elucidate interrelations among Ca^{++}, adenosine 3′,5′-monophosphate, and somatostatin. *Endocrinology* **111:** 1173–1180 (1982).
39. Cowan, J. S., B. Moor, A. Chow, and J. Kraicer. Characteristics of the post-somatostatin rebound in growth hormone secretion from perifused somatotrophs. *Endocrinology* **113:** 1056–1061 (1983).

Send reprint requests to: Dr. A. Schonbrunn, University of Texas Medical School, Department of Pharmacology, P. O. Box 20708, Houston, TX 77225.